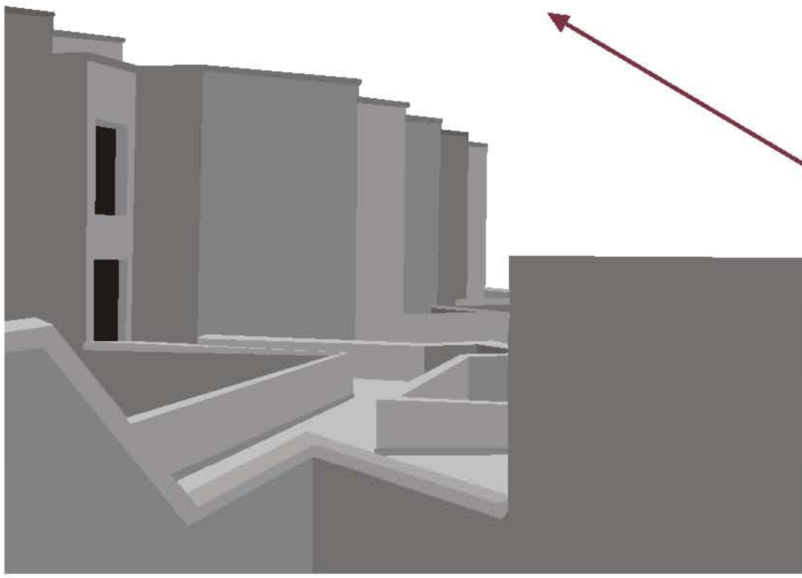

Comunicaciones del CIMAT

A NUMERICAL METHOD FOR THE INVERSE SCATTERING PROBLEM

Marcos Capistran

Comunicación del CIMAT No I-08-13/04-06-2008
(MB/CIMAT)

CIMAT

A NUMERICAL METHOD FOR THE INVERSE SCATTERING PROBLEM

MARCOS CAPISTRAN

Abstract. We propose a numerical method for the inverse scattering problem. The method is based on linearization and continuation; it iterates over frequency-increasing scattering data. Initial guesses are determined at low frequency using the convex scattering support theory of Kusiak *et al* [5]. In this paper we deal with the case a sound soft obstacle in two dimensions. The proposed method can be extended in a straightforward manner to other boundary conditions.

1. Introduction

The propagation of acoustic waves in an homogeneous isotropic medium with constant speed of sound is governed by the linear wave equation

$$U_{tt} = c^2 \Delta U \tag{1}$$

for a velocity potential U. For time-harmonic waves with frequency ω we have

$$U(x,t) = \mathrm{Re}(\mathrm{e}^{i\omega t} u(x)), \tag{2}$$

where the space dependent part $u(x)$ satisfies the Helmholtz equation

$$\Delta u + k^2 u = 0, \quad \text{for } k = \frac{\omega}{c}. \tag{3}$$

Given an obstacle of compact support $D \subset \mathbb{R}^n$ ($n = 2, 3$), its forward scattering problem is governed by the Helmholtz equation in $\mathbb{R}^n - \bar{D}$. The total wave $u(x) = \exp(ikx \cdot d) + u^s(x)$ is a superposition of the incident wave $\exp(ikx \cdot d)$ and the scattered wave $u^s(x)$,

1991 *Mathematics Subject Classification.* 78A46, 45E05, 35J05.

Key words and phrases. Inverse scattering problem, Method of continuation.

and is subject to a boundary condition on $\Gamma = \partial D$. The boundary condition can be of type

$$u = 0 \qquad \text{Dirichlet,} \tag{4}$$

$$\frac{\partial u}{\partial \nu} = 0 \qquad \text{Neumann or,} \tag{5}$$

$$\frac{\partial u}{\partial \nu} + ik\lambda u = 0 \qquad \text{impedance.} \tag{6}$$

Scattered waves u^s satisfying the Sommerfeld radiation condition

$$\lim_{r\to\infty} r^{(n-1)/2} \left(\frac{\partial u^s}{\partial r} - iku^s \right) = 0, \quad r = \|x\|_2 \tag{7}$$

are referred to as radiating solutions of the Helmholtz equation. It is known that the direct obstacle scattering problem (3)–(7) is well posed for $\Gamma \in C^2$, see [3], [4]. Given an incident wave $\exp(ikx \cdot d)$, the obstacle boundary Γ uniquely determines the scattered wave $u^s(x)$, which in turn uniquely determines the far field $u_\infty(\hat{x})$, where $(\hat{x} = \frac{x}{||x||})$. We denote by F the boundary-to-far-field mapping

$$F(\Gamma) = u_\infty(\hat{x}). \tag{8}$$

In this paper we consider the inverse problem of recovering the obstacle boundary Γ from $u_\infty(\hat{x})$, and deal with the two dimensional case with Dirichlet boundary condition. Other boundary conditions can be treated similarly.

Numerous approaches have been proposed to solve this inverse problem (see [2] or [6] for an overview). Among those, a classical approach is Newton method. Researchers have established the convergence of Newton method, see [8]. However, it is well known that problem (8) may have multiple local solutions. We propose a numerical method based on merging linearization of the problem (Newton method) with continuation on wavenumber. Initial guesses are chosen using the theory of the convex scattering support of Kusiak *et al* [5]. This is accomplished by determining the center and radius of a disk that supports the far field pattern of the scatterer boundary Γ at low wavenumber. In a second stage, the approximate solution is recursively refined at increasing wavenumbers. The paper is organized as follows. In section 2, we describe how to construct an initial guess. In section 3 we describe the method based on continuation and discuss frequency stepping and regularization. In section 4 we offer numerical evidence of the performance of the proposed method. Finally, we summarize this paper in section 5.

2. Initial guess

The following results of inverse scattering theory from [5] are required for our discussion

Definition 1. A domain D with boundary Γ supports the far field pattern u_∞ if and only if there is a radiating solution u^s of the Helmholtz equation in the exterior of $\bar{D}$ such that u_∞ corresponds to u^s.

Definition 2. The intersection of all convex domains that support u_∞ is a convex domain that supports u_∞. It is called the convex scattering support of u_∞ and is denoted $cS_k\text{supp}(u_\infty)$.

Let S_∞^D be the far field pattern operator defined by equation (34) acting on D.

According to [1], the theory of the convex scattering support is partially based on the following theorem

Theorem 3. *If the wavenumber k is such that the homogeneous Dirichlet problem for the Helmholtz equation inside D admits only the trivial solution, S_∞^D is a compact, injective operator with dense range. Furthermore, D supports the far field pattern u_∞ if and only if*

$$\sum_{p=1}^{\infty} \frac{|\langle u_\infty, g_p\rangle|^2}{\sigma_p^2} < \infty, \tag{9}$$

where $\{\sigma_p, f_p, g_p\}$ is a singular system for S_∞^D

2.1. Determination of the location of $D(x_0, \rho)$.

Bourgeois *et al* [1] study (9) for the case where D is a disk $D(x_0, \rho)$ with center x_0 and radius ρ through the following propositions

Proposition 4. *If $D = D(x_0, \rho)$, then $g_p(\theta) = \phi_m(\theta) = \frac{e^{im\theta}}{\sqrt{2\pi}}$ for $m \in \mathbb{Z}$, while the singular values σ_m are*

$$\sigma_m = \sqrt{\frac{\pi\rho}{2k}}|J_m(k\rho)|, \tag{10}$$

where J_m is the classical Bessel function of the first kind

Proposition 5. *If $S_\infty^{x_0}$ and $u_\infty^{x_0}$, respectively, denote the boundary-to-far-field mapping and the far field with source in x_0, then*

$$u_\infty \in Range(S_\infty^0) \quad \text{if and only if} \quad u_\infty^{x_0} \in Range(S_\infty^{x_0}) \tag{11}$$

Further, [1] establishes that if the scattering obstacle is a disk $D(x_0, \rho)$ with $x_0 = (x, y)$ the criterion becomes: $D(x_0, \rho)$ supports a given far field pattern u_∞ if and only if

$$\sum_{-\infty}^{\infty} \frac{|c_m|^2}{\sigma_m^2} < \infty, \tag{12}$$

where

$$c_m = \frac{1}{\sqrt{2\pi}} \int_0^{2\pi} e^{im\theta} e^{ik(x\cos(\theta)+y\sin(\theta))} u_\infty(\theta) d\theta. \tag{13}$$

$|J_m(z)|$ is a bounded oscillating function of m for $m \ll z$, and rapidly goes to zero when $m \gg z$. The moduli $|c_m|$ of the Fourier coefficients have the same behavior. Let $m_-, m_+ \in \mathbb{Z}$ such that $|c_m|$ is nearly zero for indices outside the interval (c_-, c_+). Then, we have the following remark

Remark 6. *$D(x_0, \rho)$ supports u_∞ if and only if $k\rho \geq \max(|c_-|, |c_+|)$.*

If we assume that the scattering obstacle D with far field pattern u_∞ is contained inside a large disk $D(x_1, \rho_1)$, then we can readily use remark (6) to determine the center and radius of a disk that supports u_∞ and approximates its convex scattering support $cS_k\mathrm{supp}(u_\infty)$ at low frequency.

3. A method based on continuation

The approximate solution is recursively refined by adaptive wavenumber stepping. Let Γ_j be the refinement obtained at wavenumber k_j.

Denote by

$$\delta\Gamma_j = \Gamma_{j+1} - \Gamma_j \tag{14}$$

the improvement due to the wavenumber stepping from k_j to k_{j+1}. It satisfies the linear equation

$$\frac{\partial F}{\partial \Gamma}(k_{j+1};\Gamma_j)\delta\Gamma_j = u_\infty(k_{j+1};\hat{x}) - F(k_{j+1};\Gamma_j) \tag{15}$$

to the second order of $\delta\Gamma_j$. Here, $\frac{\partial F}{\partial \Gamma}(k_{j+1};\Gamma_j)$ is the Fréchet derivative of the boundary-to-far-field mapping. The algorithm to solve the inverse scattering problem is as follows:

i) Set δk**,** δ_1**,** δ_2
ii) Initialize Γ_0**,** k_0
iii) While $||F(\Gamma_j) - u_\infty(\hat{x})||/||u_\infty(\hat{x})|| > \delta_1$
  1. Evaluate $F(k_{j+1};\Gamma_j)$**,**
  2. Evaluate $\partial F(k_{j+1};\Gamma_j)/\partial\Gamma$**,**
  3. Solve equation (15) to determine $\delta\Gamma_j$
  4. If $||F(\Gamma_j + \delta\Gamma_j) - u_\infty(\hat{x})||/||u_\infty(\hat{x})|| < \delta_2$
    Update $\Gamma_{j+1} = \Gamma_j + \delta\Gamma_j$**.**
    Update $k_{j+1} = k_j + \delta k$
  else
    Update $k_{j+1} = k_j + \frac{1}{2}\delta k$

Remark 7. *Throughout this paper we assume that the obstacle boundary* Γ *consists of one connected component. We assume that scattering data is available at all the required wavenumbers.*

3.1. **Evaluation of the boundary-to-far-field mapping.** We use standard layer potentials to evaluate to boundary-to-far-field mapping. Let

$$(S\varphi)(x) = 2\int_\Gamma \Phi(x,y)\varphi(y)ds(y), \quad x,y\in\Gamma, \tag{16}$$

$$(K\varphi)(x) = 2\int_\Gamma \frac{\partial\Phi(x,y)}{\partial\nu(y)}\varphi(y)ds(y), \quad x,y\in\Gamma, \tag{17}$$

$$(K'\varphi)(x) = 2\int_\Gamma \frac{\partial\Phi(x,y)}{\partial\nu(x)}\varphi(y)ds(y), \quad x,y\in\Gamma, \tag{18}$$

denote the single- and double-layer potentials, and the derivative of the single-layer potential, where $\Phi(x,y) = \frac{\mathrm{i}}{4}H_0^{(1)}(k\|x-y\|)$ is the Green's function of the Helmholtz equation. For simplicity, we formulate the forward scattering problem as a boundary integral equation of the first kind

$$S(\varphi)(x) = -2\mathrm{e}^{ikx\cdot d}, \tag{19}$$

where the single-layer density φ gives rise to the scattered wave u^s in $\mathbb{R}^2 - D$

$$u^s(x) = \int_\Gamma \Phi(x,y)\varphi(y)ds(y), \quad x \in \mathbb{R}^2 - D. \tag{20}$$

Now, using the asymptotic formula for the Hankel function

$$H_0^{(1)}(z) = \sqrt{\frac{2}{\pi z}}e^{i(z-\pi/4)}\left\{1 + O\left(\frac{1}{z}\right)\right\}, \quad z \to \infty, \tag{21}$$

the expansion

$$\|x-y\| = \sqrt{\|x\|^2 - 2x\cdot y + \|y\|^2} = \|x\| - \hat{x}\cdot y + O\left(\frac{1}{\|x\|}\right), \tag{22}$$

and the definition of the far field pattern $u_\infty(\hat{x})$

$$u^s(x) = \frac{\mathrm{e}^{ik\|x\|}}{\sqrt{\|x\|}}\left\{u_\infty(\hat{x}) + O\left(\frac{1}{\|x\|}\right)\right\}, \quad \|x\| \to \infty. \tag{23}$$

The boundary-to-far-field mapping may be written as

$$F(\Gamma) = u_\infty(\hat{x}) = \frac{\mathrm{e}^{ik\pi}}{\sqrt{8\pi k}}\int_\Gamma \mathrm{e}^{-ik\hat{x}\cdot y}\varphi(y)ds(y), \tag{24}$$

where the unit vector $\hat{x}$ is the outgoing direction.

3.2. **Evaluation of the derivative of the boundary-to-far-field mapping.** Let $x = x(s)$ be a parametrization with respect to arc-length $s \in [0,L]$ of the smooth simple closed curve Γ in $\mathbb{R}^2$. Let $\tau(x)$ and $\nu(x)$ be its tangent and outward normal vectors at the point $x(s)$ respectively. Perturbing Γ at each point $x \in \Gamma$ by an amount $\delta\nu(x)$ in the normal direction gives

$$\tilde{\Gamma} = \{\tilde{x} \in \mathbb{R}^2 \mid \tilde{x} = x + \delta\nu(x)\nu(x), \quad x \in \Gamma\}. \tag{25}$$

Suppose further that $\tilde{\Gamma}$ is a smooth simple closed curve in $\mathbb{R}^2$ parametrized by its arc-length $\tilde{s} \in [0, \tilde{L}]$; consequently, there is a mapping $\eta : \Gamma \to \tilde{\Gamma}$ defined by the formula

$$\eta(x) = \tilde{x} + \delta\nu(x)\nu(x). \tag{26}$$

For an element ds on Γ with endpoints $x(s)$ and $x(s + \delta s)$, the corresponding element $d\tilde{s}$ in $\tilde{\Gamma}$ is defined as the element with endpoints $\eta(x(s))$ and $\eta(x(s + \delta s))$.

Lemma 8. *Suppose Γ and $\tilde{\Gamma}$ are two smooth simple closed curves, and $\kappa(x)$ is the curvature of Γ at $x(s)$ defined by $\kappa(x) = \nu(x(s))^{\perp} \cdot \tau(x(s))$. Suppose further that $\tilde{\Gamma}$ is close to and nearly parallel to Γ; namely*

$$\kappa(x)\delta\nu(x) \ll 1, \quad \frac{d(\delta\nu)}{ds}(x) \ll 1, \tag{27}$$

then, to the second order of $\kappa(x)\delta\nu(x)$, the perturbation of the density function $\delta\nu'(x)$ satisfies

$$d\tilde{s} = (1 + \kappa(x)\delta\nu(x))ds \tag{28}$$

Proof. See [7] □

Now, let us assume that each point $x(s)$ on the boundary Γ is perturbed along the normal direction to the point $\tilde{x} = \eta(x)$. Assume further that the perturbation is small enough to satisfy the conditions from equation (27), and denote by $\tilde{\varphi}$ the solution to the integral equation on $\tilde{\Gamma}$

$$\int_{\tilde{\Gamma}} \Phi(\tilde{x}, \tilde{y})\tilde{\varphi}(\tilde{y})d\tilde{s}(\tilde{y}) = -e^{ik\tilde{x}\cdot d}. \tag{29}$$

Lemma 9. *Suppose under the conditions of lemma 8 that for $x \in \Gamma$*

$$\delta(x) = \max\{| \kappa(x)\delta\nu(x) |, |\frac{d(\delta\nu)}{ds}(x)|\} \tag{30}$$

then

$$\delta\varphi(x) = \tilde{\varphi}(\tilde{x}) - \varphi(x) \tag{31}$$

is of the first order of $\delta(x)$. Furthermore, to the second order of $\delta(x)$, $\delta\varphi(x)$ satisfies the equation

$$S(\delta\varphi+\kappa\delta\nu\varphi)(x)+K(\delta\nu\varphi)(x)+\delta\nu(x)K'(\varphi)(x) = -2ik\nu(x)\cdot de^{ikx\cdot d}\delta\nu(x) \tag{32}$$

Proof. See [7] □

The same perturbation analysis can be applied to the far field pattern. Let $\tilde{u}_\infty(\hat{x})$ be the far field pattern generated by the density function $\tilde{\varphi}$ on $\tilde{\Gamma}$ so that

$$\tilde{u}_\infty(\hat{x}) = \int_{\tilde{\Gamma}} \frac{e^{ik\pi}}{\sqrt{8\pi k}} e^{-ik\hat{x}\cdot\tilde{y}}\tilde{\varphi}(\tilde{y})d\tilde{s}(\tilde{y}), \tag{33}$$

and define

$$S_\infty(\varphi)(\hat{x}) = \frac{\mathrm{e}^{ik\pi}}{\sqrt{8\pi k}} \int_\Gamma \mathrm{e}^{-ik\hat{x}\cdot y}\varphi(y)ds(y) \tag{34}$$

Lemma 10. *Under the conditions of lemma 8, suppose φ and $\tilde{\varphi}$ are the density functions induced by Γ and $\tilde{\Gamma}$ respectively. Suppose further that u_∞ and $\tilde{u}_\infty$ are the corresponding far field patterns. Then*

$$\delta u_\infty(\hat{x}) = \tilde{u}_\infty(\hat{x}) - u_\infty(\hat{x}) \tag{35}$$

is of the first order of $\delta(x)$, and to the second order of $\delta(x)$

$$\delta u_\infty(\hat{x}) = S_\infty(-ik\hat{x}\cdot\nu\delta\nu\varphi + \delta\varphi + \kappa\delta\nu\varphi)(\hat{x}). \tag{36}$$

Proof. See [7] □

Remark 11. *In order to evaluate the Fréchet derivative of the obstacle-to-far-field mapping. We need to determine $\delta\varphi$ from equation (32) and substitute into equation (36).*

3.3. **Regularization of the linear problem.** Discretization of equation (32), leads to dense linear systems

$$Ax = b, \tag{37}$$

where A is a complex matrix with condition number $\kappa(A) \gg 1$. We propose a dynamical system approach to regularize the linear system (37) arising from the discretization of (32). Consider the dynamical system

$$\dot{x} = b - Ax, \tag{38}$$

(if A is not square positive definite we solve $\dot{z} = A^*b - A^*Az$ instead). Applying the implicit Euler method leads to

$$x_n = (I+hA)^{-1}(x_{n-1}+hb) = (I+hA)^{-n}x_0+\sum_{j=1}^{n}(I+hA)^{-j}hb \tag{39}$$

where I is the identity matrix and $h > 0$ is arbitrary.

Theorem 12. *Suppose A is a square, positive definite matrix. Let I be the identity matrix and $h > 0$ arbitrary. Then, the iterative scheme*

$$x_n = (I + hA)^{-n}x_0 + \sum_{j=1}^{n}(I + hA)^{-j}hb \tag{40}$$

converges unconditionally

Proof. Let $A = UTU^*$ be the Schur factorization of A where U is an unitary matrix and the upper triangular matrix T has diagonal elements $T_{ii} = \lambda_i > 0$, $i = 1, ..., m$ (λ_i are the eigenvalues of A in descending order). If $h > 0$, the eigenvalues of $(I + hA)^{-1}$ are $0 < (1 + h\lambda_i)^{-1} < 1$ and $(I + hA)^{-j} \to 0$ as $j \to \infty$. We conclude that the iterative scheme (40) converges unconditionally. □

Also, we conclude that the limit of x_n as $n \to \infty$ does not depend on the initial condition x_0.

Taking limit over the number of iterations we obtain

$$x^* = \lim_{n\to\infty} \sum_{j=1}^{n} (I + hA)^{-j} hb \tag{41}$$

$$= (I + hA)^{-1}(I - (I + hA)^{-1})^{-1} hb \tag{42}$$

The following lemma holds

Lemma 13. *Let A be a square positive definite matrix and $h > 0$, then*

$$A^{-1} = h(I + hA)^{-1}(I - (I + hA)^{-1})^{-1} \tag{43}$$

Remark 14. *Let $\sigma_1 \geq .. \geq \sigma_n > 0$ be the singular values of A. Since A is ill-conditioned, the smaller singular values of $I + hA$ accumulate around 1. For computational purposes we like to take $h > 0$ as large as possible. On the other hand, we must choose $h > 0$ small enough to guarantee $I + hA$ is well conditioned.*

Remark 15. *If the right hand side of the linear system (37) is noisy we implement a discrepancy principle rule (Morozov) to stop the iteration.*

4. Numerical Examples

In this section we offer numerical evidence of the performance of the method. Since a single plane incident wave will not illuminate the entire obstacle, particularly for large wavenumbers, several incident plane waves u^i_1, u^i_2, ..., u^i_l, with incident directions d^1, d^2, ..., d^l must be employed. The resulting linear systems

$$\begin{bmatrix} \frac{\partial F}{\partial \Gamma}(d^1; k_{j+1}; \Gamma_j) \\ \frac{\partial F}{\partial \Gamma}(d^2; k_{j+1}; \Gamma_j) \\ \vdots \\ \frac{\partial F}{\partial \Gamma}(d^l; k_{j+1}; \Gamma_j) \end{bmatrix} \delta\Gamma = \begin{bmatrix} u_\infty(d_1; k_{j+1}; \Gamma) - F(d^1; k_{j+1}; \Gamma_j) \\ u_\infty(d_2; k_{j+1}; \Gamma) - F(d^2; k_{j+1}; \Gamma_j) \\ \vdots \\ u_\infty(d_l; k_{j+1}; \Gamma) - F(d^l; k_{j+1}; \Gamma_j) \end{bmatrix}$$

are simultaneously solved.

Synthetic scattering data was produced solving the direct problem with a combined potential method. We used the Nystrom method to discretize the integral equations arising throughout the numerical simulations.

FIGURE 1. Five iterations suffice to reconstruct the kite-shaped obstacle although the scattering data has 1% of noise

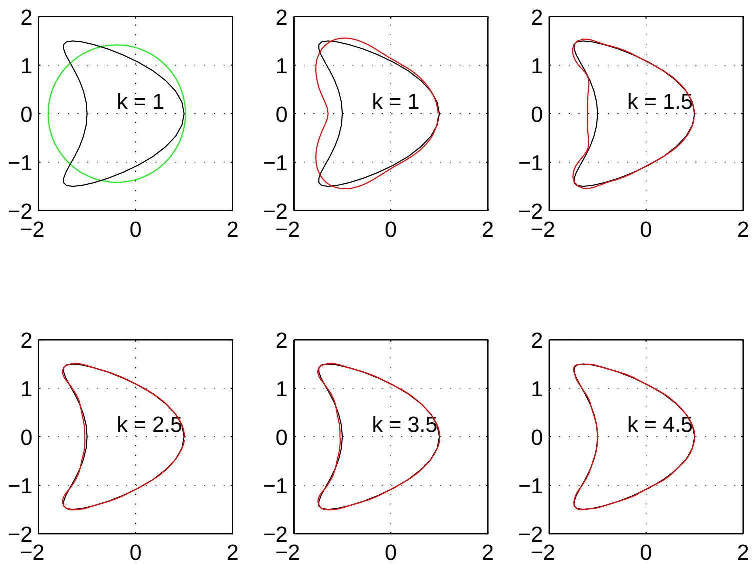

4.1. **Example.** The test consists of iterations with white noise added to the scattering data. For this example, we use a kite-shaped obstacle with boundary Γ described by the parametric representation

$$x(t) = (\cos(t) + 0.65\cos(2t) - 0.65, 1.5\sin(t)), \quad 0 \le t \le 2\pi. \tag{44}$$

In figure 1, plots were produced adding 1% of noise to the synthetic scattering data; the wavenumber of the iteration is indicated in each plot. Five steps suffice to reconstruct this kite-shaped obstacle within two significant digits. Iterations with low wavenumbers locate the scatterer while iterations with higher wavenumber reconstruct its fine details. The obstacle was probed using three incident waves with equidistant incident angles.

5. Conclusions

The numerical method introduced in this paper represents an efficient method to solve the inverse scattering problem since it can be easily modified to impedance or Neumann boundary conditions. Compared with other iterative methods it can reconstruct obstacles with high resolution at the expense of using scattering data at multiple frequencies.

References

[1] Bourgeois, L., Chambeyron, C., Kusiak, S. Locating an obstacle in a 3D finite depth ocean using the convex scattering, support *Journal of Computational and Applied Mathematics* **204** 387-99, Elsevier, (2007)
[2] Colton D., Engl H.W., Louis A.K., McLaughlin J.R. and Rundell W. *Surveys on Solution Methods for Inverse Problems* (Wien: Springer-Verlag) (2000)
[3] Colton D., Kress R., *Integral Equation Methods in Scattering Theory,* (New York: Wiley-Interscience Publications) (1983)
[4] Colton D., Kress R., *Inverse Acoustic and Electromagnetic Scattering Theory,* (New York: Springer-Verlag), (1998)
[5] Kusiak, S., Sylvester, J. The scattering support, *Communications on Pure and Applied Mathematics* **56** 1525–1548 (2003)
[6] Kress, R. Uniqueness and numerical methods in inverse obstacle scattering, *Journal of Physics: Conference Series* **71** 012003 (2007)
[7] Meyer, P.S., Capistran, M., Chen, Y. On the naturally induced sources for obstacle scattering, *Communications in Computational Physics* **1** 974-83 (2006)
[8] Potthast R., On the convergence of a new Newton-type method in inverse scattering, *Inverse Problems* **17** 1419–34

CIMAT A. C., Jalisco S/N, Valenciana, Guanajuato, GTO, 36240, MEXICO
E-mail address: marcos@cimat.mx